Optical paddle-wheel

Theodor Asavei, Vincent L.Y. Loke, Timo A. Nieminen, Norman R. Heckenberg, Halina Rubinsztein-Dunlop

The University of Queensland, School of Mathematics and Physics, Brisbane QLD 4072, Australia

ABSTRACT

As an optically trapped micro-object spins in a fluid, there is a consequent flow in the fluid.. Since a free-floating optically-driven microrotor can be moved to a desired position, it can allow the controlled application of a directed flow in a particular location. Here we demonstrate the control and rotation of such a device, an optical paddle-wheel, using a multiple-beam trap. In contrast to the usual situation where rotation is around the beam axis, here we demonstrate rotation normal to this axis.

Keywords: Two-photon photopolymerization, optical tweezers, optical torque, multiple-beam trap

1. INTRODUCTION

Two-photon photopolymerization has been proven to be a powerful technique for creating micrometer sized objects of arbitrary shape. Since its advent in 1991[1] and following the first produced 3D microstructures[2], various micromachines have been produced (micropumps, microneedles, microgears) with resolution in the order of 100 nm[3-5]. In this paper we report the design and fabrication of a micrometer sized paddle-wheel using this method. The paddle-wheel can be optically driven and moved to any position in the field of view of the microscope, which can be of interest for various biological applications where controlled application of a fluid flow is needed in a particular location and in particular direction. For example, one could imagine an experiment in which flat cells are spread out on a surface and the response to fluid flow in a plane parallel to the surface, close to the cells, is investigated.

2. PADDLE-WHEEL DESIGN AND FABRICATION

The paddle-wheel was fabricated by means of two-photon photopolymerization of UV curing resins. A detailed description of the fabrication setup and method can be found in a previous publication[6]. Essentially, micrometer sized structures can be fabricated by using 2-photon excitation of UV absorbing liquid resins. The use of 2-photon excitation instead of 1-photon is essential because in this way precise optical sectioning can be achieved and hence 3D micro-objects can be fabricated with high spatial resolution.

We used a commercially available optical adhesive, NOA63 (Norland Products Inc., NJ, USA)[7] which is a highly viscous resin that can be cured with UV light. After curing, the resin is highly transparent in the visible and near IR range making it ideal for optical tweezers experiments.

2-photon excitation is achieved by using a fs pulsed IR laser (Tsunami, Spectra Physics) with a wavelength of 780 nm.

The paddle-wheel was designed such that it could be horizontally trapped and rotated such that one could obtain a flow in a plane parallel to the rotation axis.

Trapping the paddle-wheel horizontally can be achieved by means of dual-optical tweezers if the paddle-wheel has a dumbbell shape. Once trapped a third beam could push the paddle and hence rotate it.

Figure 1 shows the 3D computer aided design of the object as well as the 2D bitmap input for the photopolymerization computer program.

Optical Trapping and Optical Micromanipulation VI, edited by Kishan Dholakia, Gabriel C. Spalding, Proc. of SPIE Vol. 7400, 740020 · © 2009 SPIE · CCC code: 0277-786X/09/$18 · doi: 10.1117/12.828426

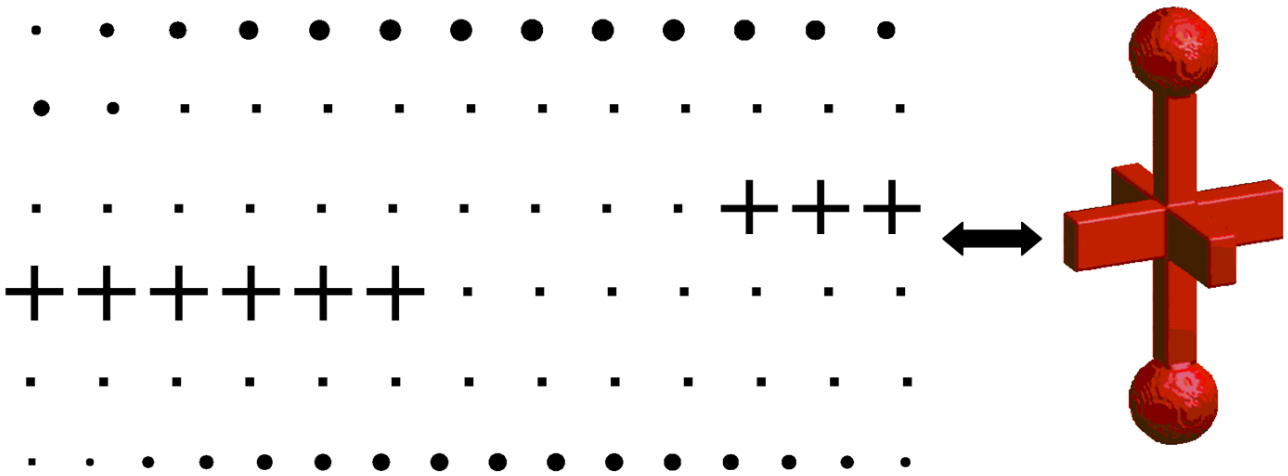

Figure 1. 3D model of the paddle-wheel and 2D bitmap slices of the object for microfabrication.

The object consists of 81 layers each separated by 200 nm in the Z direction, resulting in a length of 16 μm. The two spheres at the ends were chosen to have a diameter of 3 μm. The arms of the paddle have a length of 4 μm, a height of 2 μm and a width of 1 μm and the stalks on each side of the paddle have a 1×1 μm^2 rectangular profile.
A single micro-structure is produced in 25 minutes with a threshold photopolymerization power of 18 mW.
After photopolymerization the sample is washed with acetone in order to get rid of the unpolymerized resin. In figure 2 is shown a microfabricated paddle-wheel immediately after its fabrication and after the acetone wash.

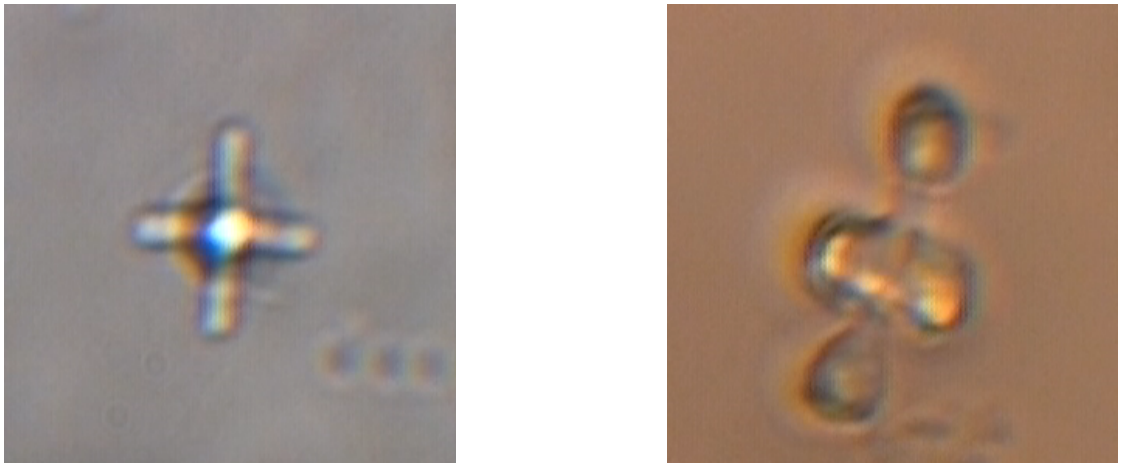

Figure 2. A bright field microscope image of a microfabricated paddle-wheel in unpolymerized resin (left) and after acetone wash (right)

The paddle-wheel is lifted from the cover slip by mechanical force, using the tip of a needle and then used in trapping and rotation experiments in water.

3. EXPERIMENTAL SETUP

The experimental setup used for trapping and rotating the paddle-wheel is based on a fully steerable dual-trap optical tweezers system[8] which allows independent movement of the trapped object in X and Y directions and most importantly in the Z direction. A scheme of the experimental setup is shown in figure 3. For dual trapping, the output from a CW Yb doped fiber laser (λ = 1070 nm, IPG Photonics) is split into two beams by means of a polarizing beam splitter cube (PBS) and then recombined through a second PBS and the two gimbal mounted mirrors (GMM) in order to enter the microscope objective.

By imaging the objective entrance aperture onto the center of each GMM by the lenses L_3 and L_4, the two traps can be steerable in the X and Y directions.

Furthermore, if an afocal telescope is placed in each of the two arms (between PBS and GMM, see figure 3) the two traps can be also moved in the Z direction.

By moving the lens L_1, the traps can be moved in the Z direction. The change in the Z position of the traps as a function of the change in the distance between L_1 and L_2 is given by[8]:

$$\Delta z = \left(\frac{f_O}{f_4}\right)^2 \left(\frac{f_3}{f_2}\right)^2 \Delta d_{12} \qquad (1)$$

where f_O is the focal length of the objective. In our configuration we find that moving L_1 by 1 cm the traps move 20 μm in the Z direction.

Rotation of the paddle-wheel is achieved by a third beam, independent of the two traps. We use the IR output from the Ti:Sapphire laser (λ = 780 nm, Tsunami, Spectra Physics) pumped by a CW solid state laser at 532 nm (Millenia, Spectra Physics).

For successful rotation of the paddle-wheel, the Ti:Sapphire laser has to be operated in CW mode. For convenience, the third beam was also steered in X and Y the same manner as described above.

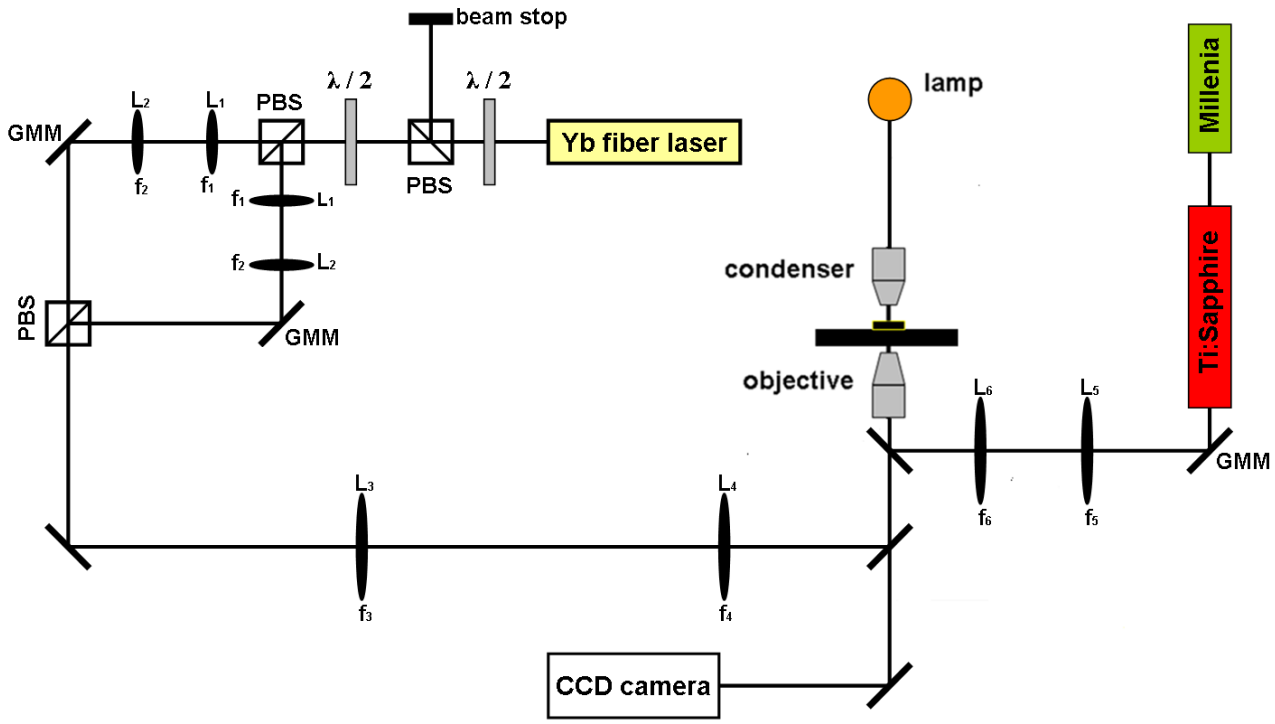

Figure 3. Schematics of the experimental setup used for trapping and rotating the paddle-wheel.

4. PADDLE-WHEEL OPTICAL ROTATION

As mentioned above, the steering in Z direction of the two traps is of importance due to the chromatic aberration of the microscope objective. We found that the difference between the focal point at 1070 nm and at 780 nm is 6 μm.
In this configuration, even if we could trap the paddle-wheel, we could not achieve any rotation from the third beam due to the large difference in Z between the foci.
Therefore, to rotate the paddle-wheel one needs to bring the foci of the three beams closer in Z direction. To do so we trap 4.5 μm polystyrene beads in the three traps and we adjust the Z position of the dual traps with respect to the "pushing" beam until all three beads are in focus. Figure 4 shows images of the three beads without and with Z steering respectively. Also, by X and Y steering we can arrange the three beams in the optimal geometry for trapping and rotation.

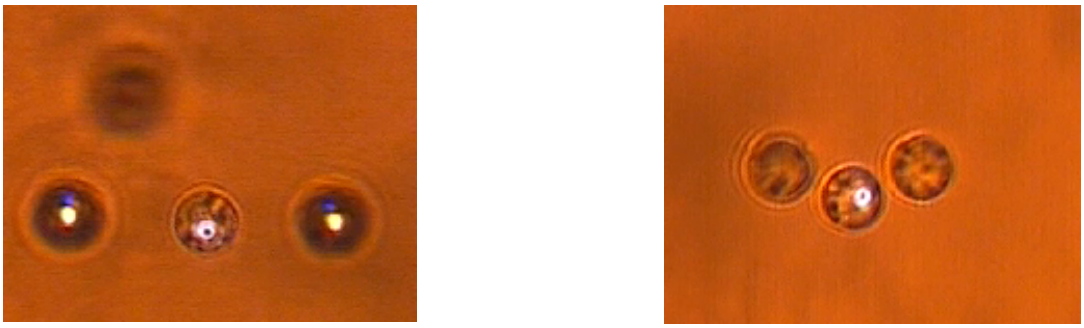

Figure 4. Optical images of polystyrene beads trapped in the three beams before (left) and after (right) Z steering of the dual trap.

In the above configuration, the trapped paddle-wheel could be rotated by the "pushing" beam impinging on the edge of the paddles as shown in the schematics of the experiment in figure 5.

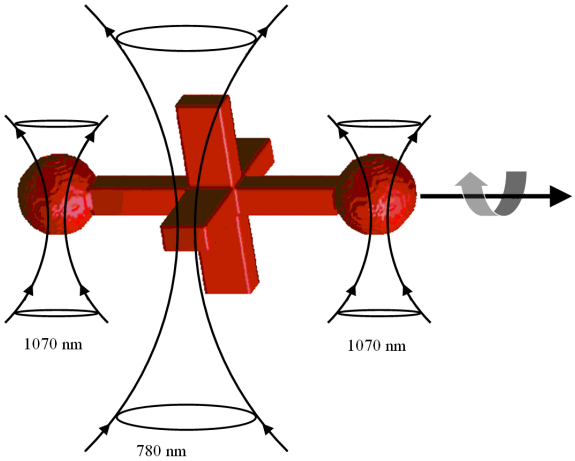

Figure 5. Schematics of the trapping and rotation of the paddle-wheel.

In figure 6 are shown consecutive frames of the rotating paddle-wheel with a rotation rate of 2 Hz. The power of the "pushing" beam was 40 mW at the sample. Knowing the rotation rate we could perform hydrodynamic simulations of the fluid flow created by the spinning paddle-wheel and could calculate the total drag torque opposing the optical torque.

Figure 6. A sequence of bright field microscope images of the rotating paddle-wheel. The frames are 14 ms apart, giving a rotation rate of 2 Hz. In the first frame the position and direction of propagation of the "pushing beam" is indicated by the marker on the paddle. The scale bar is 3 μm.

5. HYDRODYNAMIC SIMULATIONS

The fluid flow field around the rotating microstructure and hence the drag torque can be calculated from the Stokes-Navier equation which in the case of a Newtonian fluid can be written as:

$$\eta \nabla^2 \vec{v} = \nabla p \tag{2}$$

where η is the fluid viscosity and p is the hydrostatic pressure. In our case the pressure gradient is zero and equation (2) reduces to:

$$\nabla^2 \vec{v} = 0 \tag{3}$$

However, even in this simple form, the equation has an analytical solution for only a limited number of objects (sphere, spheroid, infinite cylinder). Thus in order to compare the experimental results of the optical torque with the counteracting drag torque we need to perform hydrodynamic simulations of the fluid flow generated by the rotating object of arbitrary shape.

We used the program FlexPDE (PDE Solutions Inc., Antioch, CA, USA) which is a partial differential equation solver based on finite element numerical analysis. The program constructs a tetrahedral finite element mesh over the geometry specified by the user and then solves the differential equation numerically refining the mesh and the solution until the user-defined error bound is achieved.

Thus the flow field can be simulated and the drag torque τ_d, which is the shear torque exerted by the fluid, can be found by integrating the shear stress tensor multiplied by the distance from the centre of rotation, over the rotating surface of the microstructure:

$$\tau_d = \int \sigma_{ik} x_i dA_k \tag{4}$$

where x_i is the distance in the i direction, dA_k is the surface element in the k direction and σ_{ik} is the shear stress tensor given by:

$$\sigma_{ik} = \eta \left(\frac{\partial v_i}{\partial x_k} + \frac{\partial v_k}{\partial x_i} \right) \tag{5}$$

The geometry chosen for our system was such that the microstructure was embedded in a cylinder with a diameter of 16 μm and a height of 20 μm (figure 7).

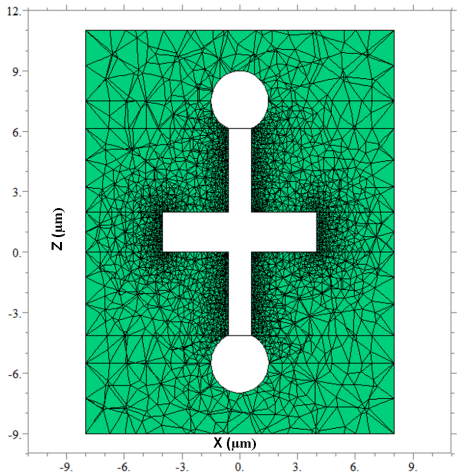

Figure 7. Cross section of the simulated surrounding medium through XZ plane.

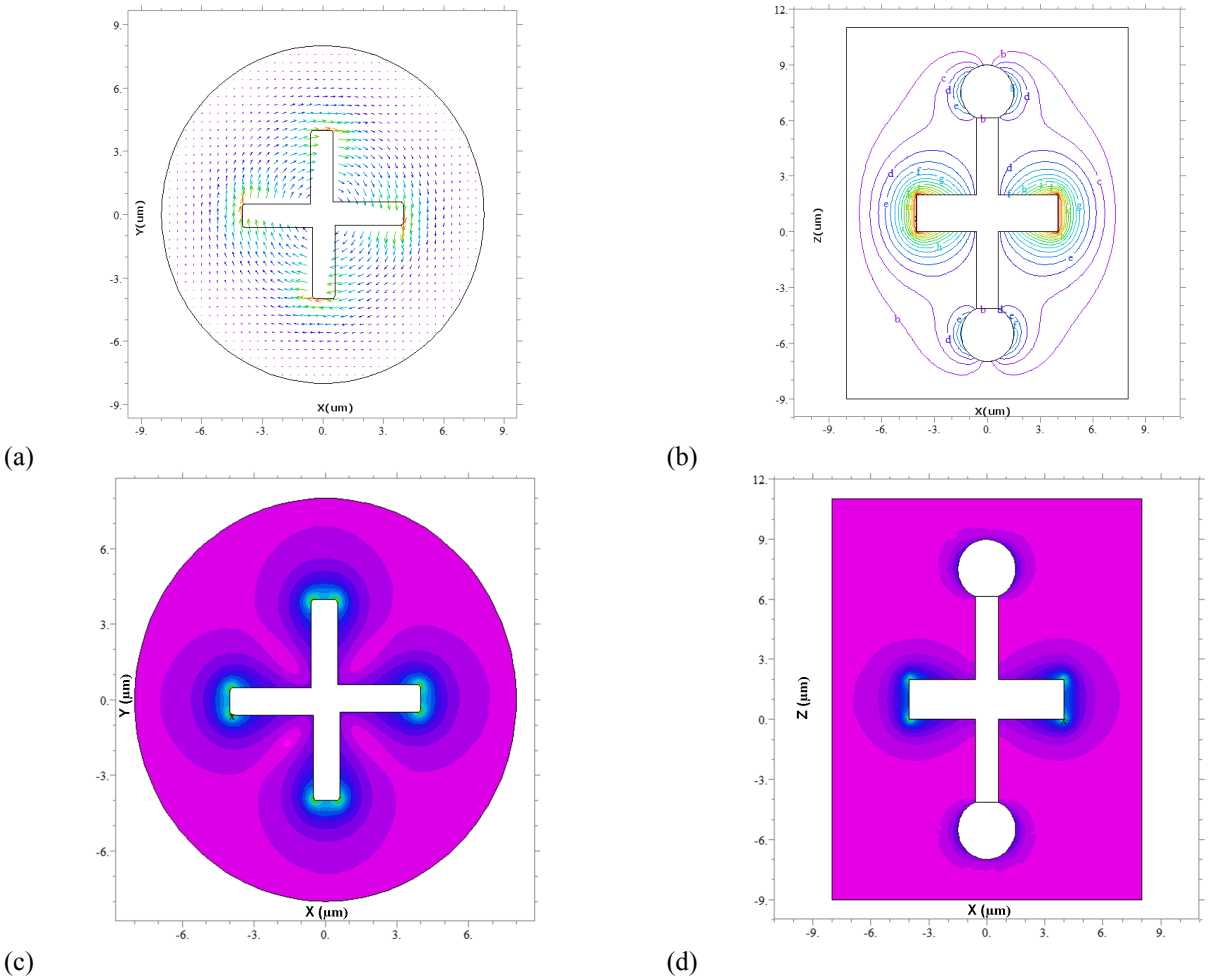

(a) (b)

(c) (d)

Figure 8. Typical graphical outputs of the FlexPDE program. Cross sections through XY (a) and XZ (b) planes respectively of the simulated flow field around the rotating particle. Similarly the cross sections through the same planes for the shear stress field are depicted in (c) and (d) respectively.

The accuracy of the method was checked by simulating the drag torque experienced by a rotating sphere in a similar geometry, for which the analytical solution of Eq. (3) is known. The difference between the simulation and the analytical solution was less than 0.5%.
Typical graphical outputs of the program are shown in figure 8 where the flow field around the rotating object is simulated as well as the shear stress field (the shear force acting per unit area) which is used to calculate the torque.
The simulated drag torque for the rotating paddle-wheel was $\tau_d = 10$ pNμm.

6. DISCUSSION AND CONCLUSION

Since the paddle-wheel is rotating with an uniform angular velocity it means that the drag torque and the optical torque due to the beam should be equal. Due to the geometry of our system we can state that the optical torque is in fact a mechanical torque due to the force created by the reflection and absorption of the "pushing" beam at the water-resin interface impinging on the arm of the paddle-wheel.
Therefore we can write:

$$\tau_o = 2n_w P\left(\frac{2R}{c} + \frac{A}{c}\right)d \tag{6}$$

where n_w is the refractive index of water, P is the power of the beam impinging on the paddle, R and A are the reflectance and absorbance at the resin water interface and d is the paddle arm.
We can neglect the torque due to the absorption due to the low absorption coefficient of the resin and we can approximate the reflectance R by:

$$R = \left(\frac{n_r - n_w}{n_r + n_w}\right)^2 \tag{7}$$

with n_r being the refractive index of the polymerized resin ($n_r = 1.56$)[7].
We obtain for the optical torque in this approximation $\tau_o = 9$ pNμm which is in good agreement with the simulated drag torque.
However, we should mention that this approximation assumed that the whole beam was at a normal incidence on the paddle. The actual "pushing" beam is highly focused (NA = 1.25) and hence in order to accurately describe the optical force, accurate simulations of the real beam need to be performed.
In conclusion, we demonstrated the fabrication and testing of an optical paddle-wheel by means of two-photon photopolymerization which proves to be a versatile tool for creating arbitrary shape 3D microstructures.

REFERENCES

[1] Strickler, J.H. and Webb, W.W. "Three dimensional optical data storage in refractive media by two-photon point excitation", Optics Letters 16, 1780-1782 (1991).
[2] Maruo, S., Nakamura, O. and Kawata, S. "Three dimensional microfabrication with two-photon absorbed photoolymerization", Optics Letters 22, 132-134 (1997).
[3] P. Galajda and P. Ormos. "Complex micromachines produced and driven by light", Applied Physics. Letters 78, 249-251 (2001).
[4] S. Maruo, K. Ikuta, and H. Korogi. "Submicron manipulation tools driven by light in a liquid", Applied Physics Letters 82, 133-135 (2003).
[5] S. Maruo and H. Inoue. "Optically driven micropump produced by three-dimensional two-photon microfabrication", Applied Physics Letters 89, 144101 (2006).
[6] Asavei, T., Nieminen, T.A., Heckenberg, N.R., and Rubinsztein-Dunlop, H. "Fabrication of microstructures for optically driven micromachines using two-photon photopolymerization of UV curing resins", Journal of Optics A 11, 034001 (2009).
[7] http://www.norlandprod.com/
[8] Fällman, E., and Axner, O. "Design for fully steerable dual-trap optical tweezers", Applied Optics 36(10), 2107-2113 (1997).